Int. J. Environ. Sci. Technol. (2014) 11:395–416
DOI 10.1007/s13762-013-0196-1

ORIGINAL PAPER

Shoreline change rate estimation and its forecast: remote sensing, geographical information system and statistics-based approach

B. Deepika · K. Avinash · K. S. Jayappa

Received: 30 December 2011 / Revised: 27 December 2012 / Accepted: 28 January 2013 / Published online: 20 February 2013

Abstract The present study indicates that coastal geomorphology is controlled by the natural processes and anthropogenic activities. The changes in shoreline positions of Udupi coast, western India, are investigated for a period of 98 years using multi-dated satellite images and topographic maps. The study area has been divided into four littoral cells and each cell into a number of transects at uniform intervals. Further, past shoreline positions have been demarcated and future positions are estimated for 12 and 22 years. The shoreline change rate has been estimated using statistical methods—end point rate, average of rates and linear regression—and cross-validated with correlation coefficient and root-mean-square error (RMSE) methods. Resultant changes from natural processes and human interventions have been inferred from the estimated values of the back-calculated errors. About 53 % of transects exhibit ±10 m RMSE values, indicating better agreement between the estimated and satellite-based shoreline positions, and the transects closer to the cell boundaries exhibit ~57 % uncertainties in shoreline change rate estimations. Based on the values of correlation coefficient and RMSE, the influence of natural processes and human interventions on shoreline changes have been calculated. The cells/transects dominated by natural processes record low RMSE values, whereas those influenced by human interventions show lower correlation coefficient and higher RMSE values. The present study manifests that the results of this study can be very useful in quantifying shoreline changes and in prediction of shoreline positions.

Keywords Coastal management · Correlation coefficient · Human intervention · Linear regression · Littoral cell · Root-mean-square error

Introduction

Coastal vulnerabilities, such as shoreline changes and coastal floods, affect the majority of coasts worldwide and are accountable for destruction of property and infrastructure. Long- and short-term shoreline changes are associated with various factors such as sediment supply, littoral transport, secular sea-level changes, hydrodynamics of nearshore environment, river mouth processes, storm surges and nature of coastal landforms (Scott 2005; Kumar and Jayappa 2009). Understanding the shoreline positions and erosion/accretion trend through time are of elemental importance to coastal scientists, engineers, and managers (Douglas and Crowell 2000; Boak and Turner 2005). Shoreline position measurements for various time periods can be used to derive quantitative estimates of rate of progradation/regradation. Due to the dynamic nature of shoreline boundary, its various indicator proxies can be used to delineate 'true' shoreline position. The shoreline indicators may be classified based on high-tide line or the wet/dry boundary, mean high water (MHW) or mean sea level (MSL), and shoreline features from remote sensing (RS) coastal images (Boak and Turner 2005). In this study, satellite images acquired during high-tide conditions have

Electronic supplementary material The online version of this article (doi:10.1007/s13762-013-0196-1) contains supplementary material, which is available to authorized users.

B. Deepika · K. S. Jayappa (✉)
Department of Marine Geology, Mangalore University, Mangalagangotri, Mangalore 574 199, Karnataka, India
e-mail: ksjayappa@yahoo.com

K. Avinash
National Centre for Antarctic and Ocean Research, Headland Sada, Vasco-da-Gama 403 804, Goa, India

been selected and during the extraction of shoreline position high-waterline has been considered as shoreline indicator.

Coastal processes in the study area are controlled by the natural processes—waves, littoral currents, offshore relief and river mouth/sea-level changes—and anthropogenic activities, such as construction of coastal structures, sand mining and dredging of navigation channels (Kumar and Jayappa 2009; Kumar et al. 2010a). Rate of change in coastal landforms and shoreline position is important in advancement of setback planning, hazard zoning, erosion/accretion perspectives, sediment budgeting, and conceptual/predictive modeling of coastal morphodynamics (Sherman and Bauer 1993; Al Bakri 1996; Zuzek et al. 2003). The shoreline change rate values represent the summaries of the processes, which have affected the coast through time, as reflected in historical shoreline position/time data (Fenster et al. 1993). Several methods—end point rate (EPR), average of rates (AOR), linear regression (LR) and jack-knifing—are being widely used to estimate and forecast the rate of change in shoreline. However, they are always subjected to uncertainty because of inherent errors and deficiencies in the model used to evaluate the historical shoreline position. Calculation of accurate shoreline change rates are frequently employed to summarize historical shoreline movements and to predict the future shoreline positions through different modeling procedures (Li et al. 2001; Appeaning Addo et al. 2008). The accuracy of shoreline change rate estimation reflects actual changes and prediction of future changes depends on several factors, such as the accuracy in shoreline position data, variability of the shoreline movement, number of measured shoreline data points (Kumar et al. 2010b), total time span of the shoreline data acquisition (Douglas et al. 1998), temporal and spatial bias in the estimation of shoreline rate-of-change statistics (Eliot and Clarke 1989), and the method used to calculate the rate (Dolan et al. 1991). In addition, causes for variation in rate of change include geomorphic features such as inlets, wave energy, engineering changes, etc. (Douglas and Crowell 2000).

Several coastal morphodynamic studies have been carried out using RS and geographical information system (GIS) techniques as they are cost-effective, reduce manual error and are useful in the absence of field surveys. The RS and GIS applications have proved effective in delineation of coastal configuration and coastal landforms, detection of shoreline positions, estimation of shoreline and landform changes, extraction of shallow water bathymetry (Jantunen and Raitala 1984; Singh 1989; White and El Asmar 1999; Lafon et al. 2002; Ryu et al. 2002; Siddiqui and Maajid 2004; Yamano et al. 2006; Kumar and Jayappa 2009; Maiti and Bhattacharya 2009; Kumar et al. 2010a).

End point rate method is an effective technique to estimate the long-term shoreline change rates by taking only two shoreline positions (i.e., early date and current) but it does not consider the variation within the time span of the record (Dolan et al. 1991). AOR method is useful for shoreline change rate studies and can yield better result when more than one shoreline position datasets are available from calculated and averaged EPR values. However, the LR method has proved to play an important role for estimating the rate of change in shoreline position, as it minimizes potential random error and short-term variability (Douglas and Crowell 2000; Allan et al. 2003; Maiti and Bhattacharya 2009). This method is also the most reliable forecaster of shoreline trends for extended intervals in the absence of physical changes such as opening of inlets or human interventions. But, the reliability of using LR method for predicting future shoreline positions decreases for the shorelines which behave in a nonlinear, cyclic, or chaotic manner (Fenster et al. 1993). In the present study, the changes in shoreline positions of Udupi coast, western India, are investigated for a period of 98 years (1910–2008) using ancillary data and satellite images. In addition, an attempt has been made to reconstruct the past and predict the future shoreline positions based on statistical methods of EPR, AOR and LR. The present work was carried out in the Department of Marine Geology, Mangalore University, India during 2010–2011.

Description of study area

The study area extends for about 60 km in the coastal zone of the Udupi district, Karnataka state from Uliyargoli in south to Yedamavina Hole inlet in north. It lies between 13°15′–13°48′N latitudes and 74°37′–74°44′E longitudes and orientated in NNW–SSE direction (Fig. 1). The coast is associated with long, narrow and straight open sandy beaches, barrier spits, estuaries, and coastal ecosystems, such as mangroves, coastal forest, and aquaculture ponds as well as major and minor industries. It is a typical open, shallow water, high-energy coast with beaches of moderate gradient (8°–16°). Six river systems that originate in Sahyadri (Western Ghats) hill ranges, a precipitous physiographic feature, debouches in single or group of two/three—Udyavara, Sita–Swarna and Kollur–Chakra–Haladi (K–C–H)—into the Arabian Sea (Fig. 1). The sediment brought by these rivers is the major source of sediment for the beaches.

The beaches of the study area are controlled and hindered by natural causes—estuarine mouths, rock exposures, source of beach material, littoral drift, wave refraction, etc.—and human interferences such as construction of >75 vented dams (a small barrier, of 5 to 7 m high, with a vent built across the river in the lower reaches for drinking water supply to the adjacent towns) across the river courses, ports/harbors, breakwaters, seawalls, revetments, etc. The area is densely populated and has a number

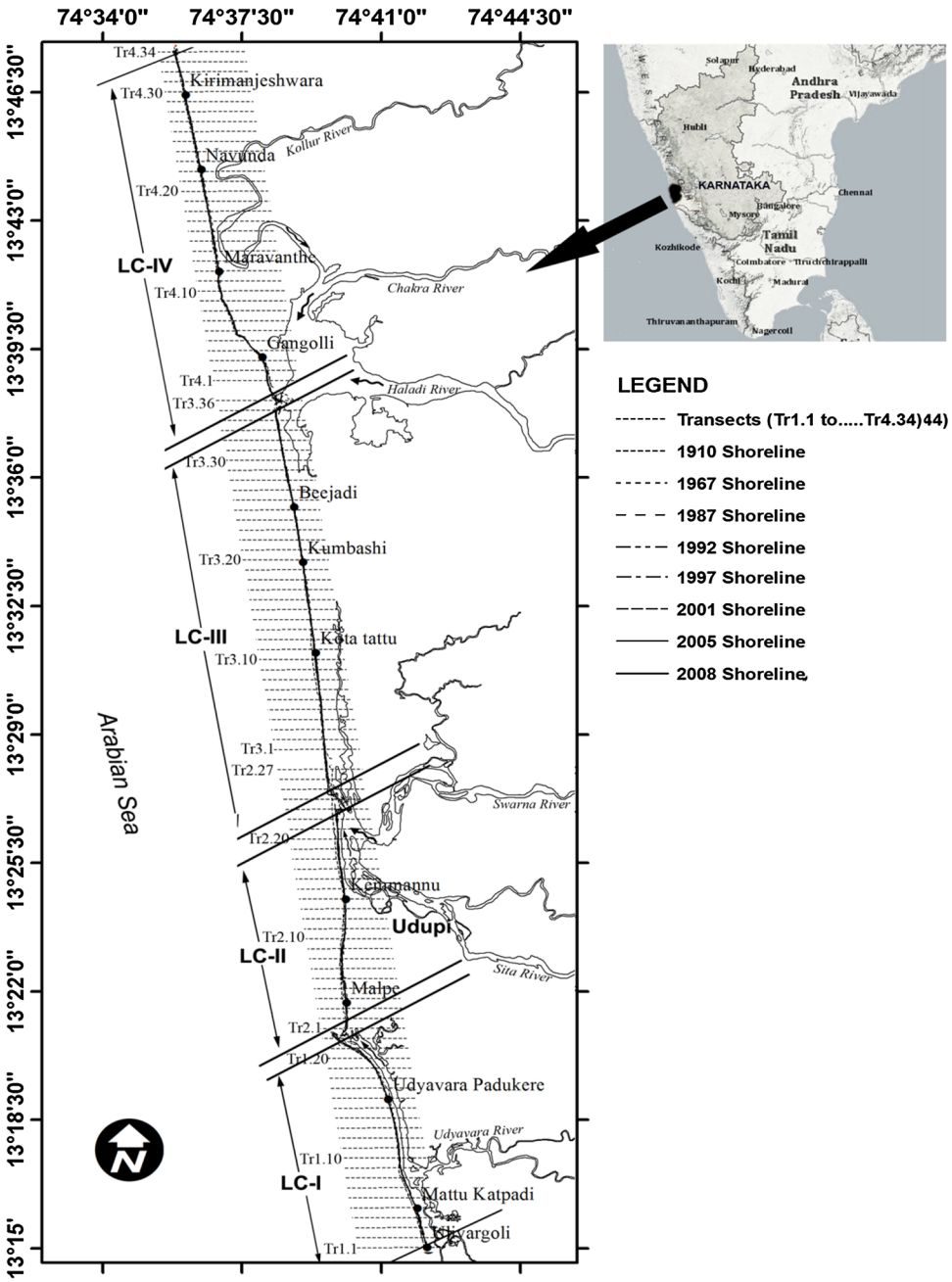

Fig. 1 Location map of the study area showing shoreline positions (during 1910–2008), transects (Tr1.1–Tr4.34), littoral cells (LC-I to LC-IV) and their boundaries

of small fishing ports. It has economic and societal significance as most of the local people depend on fishing activities.

Geology and climate

The Indian Peninsular gneissic complex (granite, granitic gneiss and migmatitic gneisses) and Bababudan Group (quartzite, chloritic phyllite, metabasites and meta-greywacke) of rocks of Archaean age are the dominant rock types in the study area (Radhakrishna and Vaidyanadhan 1994). Basic intrusives like dolerites and gabbros and acidic intrusives like pegmatite and quartz veins and pink porphyritic granites are also found. Coastal sand is found parallel to the coastline and amphibolites along the river banks. The recent alluvium and colluvial deposits occur along the riverbanks and seacoast. The exposures of crystalline rocks are found as isolated hills along the shore and in the offshore. Black clayey marine sediments with a thickness of 0.30 to >1.00 m occur as lenses along the coast. Lateritic-capped pediplains are an important physiographic feature of the study area. The district is covered

with three types of soils: (1) sandy soil—covering the beaches and the adjoining stretches, (2) yellow loamy soil—mostly along riverbanks and lower reaches of valleys, and (3) red lateritic soil—the most dominant soil type. The presence of prominent linear beach ridges and swales between Udupi and Kundapur indicates progradation of coast in this sector. Offsetting of the straight-line coast, acute bends in stream courses and minor differences in elevation on either side of the beach ridges are evidences of neo-tectonic activity in the study area. Deccan trap rocks with unique development of columnar joints found at St. Mary's island off the Udupi coast have been declared as a National Geological Monument (Abbas et al. 1991).

The study area experiences a typical maritime climate with an average temperature of 26.5 °C. The winds are mainly westerly or southwesterly and strong during the southwest (summer) monsoon. The average annual rainfall is 4,100 mm, of which about 80 % is received during the southwest monsoon and the remainder during the northeast (winter) and inter-monsoon months (Kumar et al. 2010a). Significant wave height (Hs) of the area during non-monsoon months is 1.5 m while during monsoon months, it is >3.5 m. Tides are semi-diurnal with a mean tidal range of 1.2 m and spring tidal range of 1.8 m (SOI 2007). Wave breaker height, average surf zone width and wave period of the region are 0.5–2.8, 15–100 m, 7–15 s, respectively (Vijaya Kumar 2003).

Materials and methods

In the present study, RS, GIS and statistical techniques have been used to evaluate the shoreline change rate and cross-validation with root-mean-square error technique as suggested by Fenster et al. (1993), Allan et al. (2003), Maiti and Bhattacharya (2009), and Kumar et al. (2010b). Future shoreline positions for 12 and 22 years with reference to 2008 as the base year are predicted, based on the estimated shoreline change rates. Topographic maps and multi-spectral satellite images have been utilized to demarcate the shoreline positions of different periods (Table 1). Shoreline positions of different time periods have been digitized accurately by taking high-water line (HWL) into consideration. The vector layers were superimposed and overlay analyses of shoreline changes were carried out to estimate the area of erosion and accretion between 1910 and 2008 period. The study area has been divided into four littoral cells (LCs) (LC-I to LC-IV) and then, LCs were further divided into number of transects (Tr1.1, Tr1.2,…, Tr1.*n*) (Fig. 1). Shoreline change rates were estimated at each transects using three different statistical methods, namely EPR, AOR and LR (Table 2). To estimate the inaccuracies/uncertainty in shoreline change rate and cross-validate, the computed past shoreline positions, correlation coefficient (*R*) and RMSE, respectively, were considered. Estimated rates of shoreline change are used to predict the future shoreline positions using EPR and LR models. Resultant changes from natural processes and human intervention have been inferred from the estimated values of the back-calculated errors. For the entire study area, the transect-wise shoreline change rates have been calculated and are given in Table 2.

Data analysis and geo-rectification

Different data products such as the Survey of India (SOI, 2007) topographic maps of 1910, 1967 and 1987 editions (1:63,360, 1:50,000, 1:25,000 scales, respectively); Landsat 5 TM image of 1992 (30 m spatial resolution); and Indian remote sensing (IRS)—1C and P6 linear self scanning (LISS-III, 23.5 m resolution) images of 1997, 2001, 2005 and 2008 were employed in this study. To calculate the short- as well as the long-term shoreline changes, various datasets of eight different periods have been

Table 1 Details of the satellite data products, date and time of acquisition, tidal conditions and the amount of shoreline shift

Sensor	Time (GMT +5:30)	Date of acquisition	Tide condition			LC-wise total amount of shoreline shift (m)			
			Tidal height (m)	Condition	SL shift from HT (m)	Katapadi LC-I (10)[a]	Malpe LC-II (8)[a]	Saligrama LC-III (7)[a]	Maravanthe LC-IV (12)[a]
IRS-P6	05:35:48	14-January-2008	0.76	Rising	0.87	8.7	6.96	6.09	10.44
IRS-P6	05:36:10	7-December-2005	1.36	Rising	0.50	5.0	4.00	3.50	6.00
IRS-1C	05:31:50	4-December-2001	1.27	Rising	0.48	4.8	3.84	3.36	5.76
IRS-1C	05:40:47	23-January-1997	1.40	Rising	0.08	0.8	0.64	0.56	0.96
Landsat5 TM	03:38:00	1-April-1992	2.28	Rising	0.8	8.0	6.4	5.6	9.6

SL sea level, *HT* high tide, *LC* littoral cell

[a] Beach slope in degrees

Table 2 Shoreline change rate (m/year), correlation coefficient (*R*), cross validated RMS error (11- and 21-years), predicted future shoreline positions (m) for the period 1910–2008 using EPR and LR methods

Transect no.	Rate (m/year)			*R*	Back-calculated RMS error (m)		Future prediction by EPR (m)		Future prediction by LR (m)		Geomorphologic features/field observations
	EPR	AOR	LR		11 years (1997)	21 years (1987)	12 years (2020)	22 years (2030)	12 years (2020)	22 years (2030)	
LC-I (between Uliyargoli and Udyavara river mouth)											
Tr1.1	−0.86	−0.98	−1.25	0.76	14.44	48.09	−95.14	−103.79	−121.60	−134.09	Erosion-prone beach (Uliyargoli), protected with seawall
Tr1.2	−1.11	−1.21	−1.31	0.80	11.87	67.80	−122.55	−133.69	−137.90	−151.00	
Tr1.3	−0.69	−1.00	−1.02	0.68	15.41	64.32	−75.72	−82.61	−111.62	−121.83	
Tr1.4	−0.65	−1.22	−1.22	0.76	6.92	41.62	−71.80	−78.32	−134.50	−146.72	Receding open beach (Tr1.4–Tr1.11)
Tr1.5	−1.28	−1.32	−1.47	0.90	17.45	31.09	−140.32	−153.07	−152.97	−167.67	
Tr1.6	−1.16	−0.95	−1.21	0.77	8.47	41.18	−127.99	−139.62	−116.71	−128.78	Eroding beach; rock outcrops are present
Tr1.7	−1.25	−1.14	−1.46	0.85	9.32	31.09	−137.44	−149.94	−140.42	−155.04	Maximum rate of recession noticed
Tr1.8	−1.09	−0.90	−1.12	0.78	2.08	45.46	−120.08	−131.00	−110.56	−121.72	Beach (Tr1.8–Tr1.21) lies on Udayavara spit
Tr1.9	−0.72	−0.44	−0.72	0.64	13.21	37.52	−79.17	−86.37	−62.86	−70.08	Open beach
Tr1.10	−0.26	−0.03	−0.14	0.25	30.40	18.87	−28.18	−30.74	−9.14	−10.53	
Tr1.11	−0.10	−0.07	−0.12	0.21	40.51	9.05	−10.92	−11.92	−11.09	−12.31	
Tr1.12	−0.01	0.16	0.10	0.24	25.29	10.57	−1.11	−1.21	14.56	15.58	
Tr1.13	0.25	0.41	0.31	0.53	27.57	15.70	27.03	29.49	40.15	43.23	Stable beach from Tr1.13 to Tr1.18
Tr1.14	0.32	0.38	0.42	0.84	9.33	11.81	35.59	38.83	44.76	48.98	
Tr1.15	0.48	0.56	0.48	0.87	3.63	15.76	53.25	58.09	57.42	62.24	
Tr1.16	1.21	1.37	1.07	0.85	4.87	3.41	132.92	145.00	135.80	146.50	Backshore is protected by mangroves & Ipomoea—a sand binder
Tr1.17	1.55	1.90	1.36	0.75	4.01	16.67	170.98	186.52	183.35	196.98	Maximum rate of progradation is recorded
Tr1.18	0.55	0.80	0.49	0.58	15.16	3.29	60.83	66.36	72.62	77.51	
Tr1.19	0.39	0.38	0.27	0.39	7.13	2.21	42.78	46.67	36.21	38.86	Beach configuration (Tr1.19–Tr1.21) is influenced by group of islands situated in the offshore
Tr1.20	−0.35	−0.71	−0.63	0.55	11.35	50.57	−38.40	−41.89	−74.28	−80.60	
Tr1.21	−0.62	−1.67	−1.19	0.41	5.25	167.38	−67.88	−74.05	−162.83	−174.69	
Tr1.22	1.40	0.72	1.20	0.67	50.32	62.07	153.85	167.84	101.67	113.67	Growth of southern spit after construction of the breakwater on either side of the Udyavara river mouth in 1980s
LC-II (between Udyavara river mouth and Sita–Swarna rivers mouth)											
Tr2.1	−1.04	−1.63	−1.07	0.68	17.78	29.41	−113.85	−124.20	−153.12	−163.85	Breakwater at the mouth of river mouth acting as barrier for littoral drift
Tr2.2	−0.56	−1.08	−0.86	0.67	24.60	10.21	−61.09	−66.64	−109.57	−118.17	Malpe harbour; tourist spot; rock outcrops are present
Tr2.3	−1.53	−1.74	−1.49	0.89	8.98	49.83	−168.40	−183.71	−179.44	−194.37	
Tr2.4	−1.74	−1.81	−1.86	0.83	20.63	84.62	−191.54	−208.95	−202.01	−220.60	Beach configuration is influenced by St. Mary's group of islands situated in the offshore
Tr2.5	−1.09	−1.73	−1.55	0.78	28.88	79.83	−120.24	−131.17	−182.26	−197.78	

Table 2 continued

Transect no.	Rate (m/year)			*R*	Back-calculated RMS error (m)		Future prediction by EPR (m)		Future prediction by LR (m)		Geomorphologic features/field observations
	EPR	AOR	LR		11 years (1997)	21 years (1987)	12 years (2020)	22 years (2030)	12 years (2020)	22 years (2030)	
Tr2.6	−0.76	−1.19	−1.13	0.66	48.16	60.52	−83.23	−90.80	−128.00	−139.31	Opening of a new small inlet in between 1910 and 1967
Tr2.7	−0.87	−1.03	−0.92	0.81	20.30	36.82	−96.10	−104.84	−107.90	−117.09	
Tr2.8	−0.82	−0.89	−0.40	0.30	4.28	37.16	−90.56	−98.80	−74.49	−78.51	
Tr2.9	−0.72	−0.90	−0.35	0.23	17.84	39.45	−79.54	−86.77	−72.82	−76.36	Progradation and recession is a cyclic phenomenon
Tr2.10	−1.18	−1.55	−1.07	0.75	3.19	17.29	−129.48	−141.25	−148.28	−159.01	
Tr2.11	−1.04	−1.09	−0.86	0.78	4.99	18.48	−114.20	−124.58	−108.73	−117.35	
Tr2.12	−1.01	−1.21	−1.03	0.80	5.19	29.07	−110.64	−120.70	−124.21	−134.54	Open beach
Tr2.13	−0.54	−0.67	−0.66	0.66	1.99	19.18	−59.54	−64.96	−72.45	−79.06	
Tr2.14	−0.82	−0.70	−0.77	0.69	1.66	24.86	−90.03	−98.22	−81.42	−89.15	Severely eroding Kemmannu beach; seawalls are partially collapsed
Tr2.15	−0.61	−0.73	−0.62	0.67	0.98	24.65	−66.64	−72.70	−74.53	−80.72	
Tr2.16	−0.69	−1.17	−0.98	0.78	8.84	30.28	−75.88	−82.78	−119.92	−129.75	Lies (Tr2.16–Tr2.22) on Oddu Bengre spit
Tr2.17	−0.80	−1.24	−1.14	0.84	4.02	32.73	−88.17	−96.18	−132.10	−143.48	
Tr2.18	−1.24	−1.58	−1.30	0.85	5.25	25.86	−136.41	−148.81	−160.95	−173.99	Partially collapsed seawalls
Tr2.19	−1.57	−1.54	−1.35	0.84	4.45	43.55	−172.53	−188.22	−160.47	−173.92	
Tr2.20	−1.52	−1.59	−1.55	0.95	19.47	21.43	−167.16	−182.35	−173.86	−189.36	
Tr2.21	−1.58	−1.54	−1.87	0.86	13.13	28.18	−173.35	−189.11	−185.87	−204.52	Protected with seawall
Tr2.22	−1.97	−2.25	−1.86	0.83	10.24	17.12	−216.82	−236.53	−228.82	−247.42	
Tr2.23	−2.45	−2.43	−2.43	0.60	72.87	57.86	−269.33	−293.82	−267.76	−292.04	Maximum rate of recession is noticed near the river mouth
Tr2.24	–	−0.23	−0.05	0.04	15.92	103.20	–	–	−17.10	−17.62	Major shift of Sita–Swarna rivers mouth toward south by ~2.30 km is recorded in last 98 years
LC-III (between Sita–Swarna rivers mouth and Kollur–Chakra–Haladi rivers mouth)											
Tr3.1	−0.25	−0.03	−0.10	0.14	18.94	11.90	−27.77	−30.30	−6.50	−7.47	Lies on Kodi Bengre spit
Tr3.2	−0.08	0.13	−0.21	0.24	4.40	6.38	−8.51	−9.28	−3.05	−5.10	
Tr3.3	0.11	0.17	0.00	0.00	14.66	21.33	12.05	13.15	10.33	10.33	Protected with seawall
Tr3.4	0.24	0.43	0.25	0.28	6.76	25.36	26.83	29.27	38.47	40.97	
Tr3.5	−0.15	0.04	−0.24	0.26	0.48	26.32	−16.65	−18.17	−10.16	−12.56	
Tr3.6	−0.01	0.37	0.04	0.05	1.82	19.55	−0.62	−0.68	24.67	25.04	Open beach; sand dune in the hinterland (about a kilometer away from the shoreline)
Tr3.7	−0.94	−1.22	−0.98	0.84	17.87	6.53	−103.39	−112.78	−122.93	−132.74	
Tr3.8	−1.24	−1.48	−1.30	0.89	25.59	0.64	−136.50	−148.91	−153.32	−166.30	
Tr3.9	−1.61	−1.75	−1.51	0.87	0.16	18.45	−176.80	−192.87	−180.92	−196.02	
Tr3.10	−1.71	−1.75	−1.51	0.87	2.85	20.29	−187.80	−204.88	−181.14	−196.28	Open beach; seawalls are collapsed; maximum rate of recession recorded
Tr3.11	−1.06	−1.40	−1.10	0.73	6.45	25.12	−117.09	−127.74	−138.92	−149.88	
Tr3.12	−1.02	−1.27	−1.04	0.77	6.59	29.91	−112.20	−122.39	−128.15	−138.58	Protected with seawall
Tr3.13	−0.43	−0.53	−0.38	0.55	7.20	30.97	−47.18	−51.47	−50.51	−54.33	
Tr3.14	−0.16	−0.11	−0.09	0.20	4.44	26.73	−17.62	−19.23	−11.24	−12.18	
Tr3.15	−0.06	−0.04	0.12	0.21	26.28	15.55	−6.57	−7.17	3.18	4.41	
Tr3.16	0.15	0.01	0.36	0.36	12.39	3.88	16.72	18.24	17.71	21.34	Stable beach

Table 2 continued

Transect no.	Rate (m/year)			*R*	Back-calculated RMS error (m)		Future prediction by EPR (m)		Future prediction by LR (m)		Geomorphologic features/field observations
	EPR	AOR	LR		11 years (1997)	21 years (1987)	12 years (2020)	22 years (2030)	12 years (2020)	22 years (2030)	
Tr3.17	−0.20	−0.62	−0.24	0.27	18.35	5.06	−21.51	−23.47	−50.79	−53.23	
Tr3.18	−0.09	−0.51	−0.15	0.19	21.55	1.76	−10.41	−11.35	−38.05	−39.57	
Tr3.19	0.12	−0.17	−0.03	0.09	3.33	3.11	12.69	13.84	−12.08	−12.42	
Tr3.20	0.12	−0.39	−0.17	0.23	5.92	10.26	13.48	14.71	−31.84	−33.56	
Tr3.21	0.19	0.01	0.20	0.32	16.79	8.93	20.95	22.85	9.77	11.81	Eroding beach; properly constructed seawalls; small inlets are joining the sea
Tr3.22	−0.01	−0.28	−0.05	0.07	23.25	4.13	−0.88	−0.96	−19.77	−20.22	
Tr3.23	−0.10	−0.33	−0.11	0.18	23.08	11.44	−11.54	−12.59	−25.09	−26.23	Organic shells extraction is done
Tr3.24	0.00	0.02	0.14	0.27	1.13	17.46	0.54	0.58	7.39	8.83	
Tr3.25	−0.13	−0.15	0.01	0.01	3.48	4.12	−14.17	−15.45	−8.49	−8.41	Open beach; Casuarina trees at the backshore
Tr3.26	0.04	−0.02	0.09	0.19	7.71	9.74	4.86	5.31	3.46	4.35	
Tr3.27	0.03	−0.26	−0.11	0.19	12.90	11.05	3.45	3.76	−21.65	−22.72	
Tr3.28	0.06	−0.51	−0.31	0.38	10.07	6.93	6.12	6.67	−47.16	−50.23	
Tr3.29	−0.03	−0.41	−0.32	0.46	27.50	17.70	−3.31	−3.61	−40.36	−43.58	
Tr3.30	0.44	0.38	0.33	0.60	11.14	26.77	48.75	53.18	39.33	42.65	Lies (Tr3.30–Tr3.35) on Kasaba Kodi spit (southern)
Tr3.31	0.24	0.16	0.08	0.12	3.65	7.69	26.23	28.61	13.45	14.25	
Tr3.32	−0.08	−0.01	−0.09	0.15	13.44	6.13	−8.28	−9.04	−4.95	−5.81	
Tr3.33	−0.20	0.21	−0.01	0.01	9.05	14.82	−22.24	−24.26	12.79	12.72	Sand mining is observed
Tr3.34	−0.14	0.17	−0.04	0.08	8.10	5.38	−15.55	−16.97	8.18	7.76	
Tr3.35	0.02	0.16	−0.12	0.10	27.17	50.83	2.42	2.64	4.72	3.52	Southern spit has been reduced toward south by ~700 m; width of the K–C–H rivers mouth has been reduced
LC-IV (between Kollur–Chakra–Haladi rivers mouth and Yedamavina hole inlet)											
Tr4.1	0.80	0.88	1.18	0.77	0.59	16.30	88.22	96.24	112.16	123.95	Lies on the tip of the Gangolli spit
Tr4.2	0.90	0.92	0.99	0.81	0.53	21.12	99.40	108.44	104.26	114.11	Gangolli harbour
Tr4.3	0.79	0.76	0.80	0.75	11.52	19.50	86.45	94.31	85.71	93.71	
Tr4.4	−0.48	−0.31	−0.45	0.47	12.50	2.06	−52.83	−57.63	−41.52	−46.04	Rock exposures (Tr4.4–Tr4.7)
Tr4.5	−0.13	−0.14	−0.26	0.52	16.82	5.06	−14.57	−15.89	−21.54	−24.11	Rocky shore; light house is present
Tr4.6	−0.87	−0.79	−0.78	0.80	8.41	24.05	−95.25	−103.91	−86.03	−93.86	
Tr4.7	−0.70	−0.74	−0.64	0.81	0.16	26.20	−76.93	−83.92	−77.11	−83.48	
Tr4.8	−0.54	−0.64	−0.57	0.63	0.72	40.34	−59.89	−65.33	−65.94	−71.62	
Tr4.9	−0.81	−0.82	−0.68	0.67	9.35	45.77	−89.56	−97.70	−83.01	−89.77	Rock exposures
Tr4.10	0.08	0.01	0.02	0.03	9.57	37.17	8.87	9.68	2.12	2.35	
Tr4.11	0.39	0.15	0.50	0.43	12.84	36.35	43.12	47.04	32.89	37.90	Open beach
Tr4.12	−0.33	−0.63	−0.30	0.30	11.62	15.93	−35.94	−39.20	−53.70	−56.66	
Tr4.13	−0.38	−0.74	−0.37	0.37	1.11	17.10	−41.43	−45.20	−63.15	−66.80	
Tr4.14	−0.60	−0.85	−0.54	0.48	6.89	40.52	−66.14	−72.15	−79.06	−84.47	Severely eroding beach; seawalls are partially collapsed; Kollur river is running parallel to the beach
Tr4.15	−0.49	−0.82	−0.53	0.51	11.36	30.26	−53.54	−58.41	−75.68	−80.93	

Table 2 continued

Transect no.	Rate (m/year)			*R*	Back-calculated RMS error (m)		Future prediction by EPR (m)		Future prediction by LR (m)		Geomorphologic features/field observations
	EPR	AOR	LR		11 years (1997)	21 years (1987)	12 years (2020)	22 years (2030)	12 years (2020)	22 years (2030)	
Tr4.16	−0.16	−0.34	−0.04	0.04	11.80	35.23	−17.39	−18.97	−22.91	−23.33	
Tr4.17	0.33	0.19	0.45	0.52	2.79	23.31	36.45	39.76	33.50	38.03	Tourist spot
Tr4.18	0.24	−0.02	0.32	0.39	7.97	7.54	26.33	28.72	13.54	16.76	
Tr4.19	0.07	−0.09	0.21	0.24	8.66	16.61	7.16	7.81	4.29	6.42	
Tr4.20	−0.32	−0.44	−0.06	0.06	2.44	34.83	−35.17	−38.37	−29.93	−30.55	Severely eroding beach; protected with seawalls
Tr4.21	−0.36	−0.86	−0.52	0.47	8.77	27.73	−39.40	−42.98	−77.29	−82.51	
Tr4.22	−0.47	−0.96	−0.57	0.52	9.17	19.49	−51.60	−56.29	−87.37	−93.06	
Tr4.23	−0.62	−0.94	−0.63	0.60	7.58	32.32	−67.89	−74.06	−88.47	−94.79	Open beach
Tr4.24	−0.34	−0.81	−0.43	0.42	13.93	16.09	−37.68	−41.10	−70.28	−74.61	
Tr4.25	−0.67	−0.80	−0.67	0.80	10.92	14.90	−74.21	−80.96	−82.24	−88.94	
Tr4.26	−0.33	−0.56	−0.40	0.41	3.26	36.48	−36.80	−40.15	−52.53	−56.49	Wide beach; protected with seawall; small seasonal streams in the vicinity
Tr4.27	−0.59	−0.77	−0.56	0.61	5.37	21.75	−64.98	−70.89	−73.42	−79.04	
Tr4.28	−0.47	−0.71	−0.48	0.55	11.54	9.02	−52.03	−56.76	−67.22	−71.97	
Tr4.29	−0.46	−0.77	−0.62	0.68	13.79	2.21	−50.66	−55.27	−77.85	−84.05	Rock exposures
Tr4.30	−0.44	−0.70	−0.42	0.49	6.94	2.31	−48.48	−52.89	−64.25	−68.44	Stable beach
Tr4.31	−0.55	−0.76	−0.58	0.73	8.89	6.03	−60.15	−65.61	−74.38	−80.18	
Tr4.32	−0.18	−0.53	−0.26	0.34	19.40	2.22	−19.41	−21.17	−44.70	−47.28	Open beach
Tr4.33	0.26	−0.02	0.26	0.28	2.77	23.61	28.06	30.62	11.26	13.89	
Tr4.34	0.44	−0.27	0.20	0.12	49.43	10.32	48.69	53.12	−8.52	−6.53	Near to Yedamavina hole inlet

Negative sign indicates erosion

selected between 1910 and 2008, based on their availability. The details of satellite data products and their acquisition, tidal conditions, and computed shoreline shift are given in Table 1.

The satellite images have been geometrically corrected using ERDAS v.9.1 software. The SOI topographic map of 1967 has been taken as reference map for geo-rectification. More than 50 ground control points (GCPs) were selected on the satellite image as well as on the topographic map to derive a polynomial transformation of the first (affine) order. Horizontal accuracy of less than 0.3 pixels (about 10 m on ground) was achieved. RMSE has taken into account both during image-to-image and image-to-map geometric corrections. After geo-rectification, a nearest neighbour interpolation method (as no change occurs to the pixel values) was used to rectify and resample the images into a universal transverse mercator (UTM) projection, Zone 43 North (Kumar et al. 2010a).

The potential shoreline position error among the multi-dated satellite images due to tidal variation, weather conditions and pixel variations during data acquisition have been optimized in the present study. In this method satellite images were gridded uniformly and the normal sea conditions and beach width were taken into account in the selection of the best grid resolution as suggested by Gourlay (1996), Hengl (2006) and Kumar et al. (2010b).

Selection of littoral cells and transects

Littoral cells are defined as relatively self-contained units within which sediment circulates and essential in identifying the discontinuities in rate or direction of sediment transport (Bray et al. 1995). It is also used to understand the interaction processes and management of shoreline at the regional scale. The coastal stretch of study area has been broadly divided into four LCs (LC-I to LC-IV) which have similar sedimentary and hydrodynamic characteristics (Fig. 1). The cell boundaries have been demarcated based on stability of river/estuarine inlets, rock exposures, spits, major/minor ports (Malpe and Gangolli) and artificial structures. The boundaries of the four LCs are: (1) LC-I of 11 km, between the Uliyargoli and Udyavara river mouth; (2) LC-II of 13.5 km, between the Udyavara river mouth and Sita–Swarna rivers mouth; (3) LC-III of 18 km,

between the Sita–Swarna rivers mouth and K–C–H rivers mouth; (4) LC-IV of 17 km, between K–C–H rivers mouth and Yedamavina Hole inlet. For high-resolution accurate studies, each littoral cell has been further divided into different transects (Tr1.1 to Tr4.34) with uniform interval of 500 m, oriented perpendicular to the baseline.

Shoreline change rate calculations and predictions

The shoreline position of 1910 was considered as a reference line or zero (0) position to find out the significant trend in the rate of shoreline change at all transects. With reference to this baseline, progradation of the shoreline is considered as a positive value, while recession as a negative value. The shoreline calculation and prediction techniques allow the stability of a long-term trend relative to intermediate (>50 years) and short-term (decennial) trends, thereby best relating to the past with expected future shoreline positions. In this study, three different methods, such as EPR, AR and LR, have been used to calculate the shoreline change rate and its forecast. Details of the methods used are discussed below.

End point rate

End point rate is calculated by dividing the distance of total shoreline movement by the time elapsed between the earliest and latest measurements at each transect. The future shoreline position for a given date is estimated using the rate and intercept (Fenster et al. 1993):

$$Y = mX + B \tag{1}$$

where Y denotes shoreline position, X for date, B for the intercept, and m for rate of shoreline movement. Given shoreline datasets, numbered in ascending order by date, the EPR intercept is:

$$B_{\mathrm{EPR}} = Y_n - m_{\mathrm{EPR}} \times X_n \tag{2}$$

Average of rates

To incorporate the accuracy of the shoreline position data and magnitude of the rate of change, Foster and Savage (1989) developed an equation to determine whether any given EPR meets a minimum time criterion (T_{min}):

$$\frac{\sqrt{(E_1)^2+(E_2)^2}}{R_1} \tag{3}$$

where E_1 and E_2 are the measurement errors in the first and second point, respectively, and R_1 is the EPR of the longest time span for a particular transect.

Advantage of using AOR is that all the EPRs that survive the minimum time span equation are used and allows calculation of the time-dependent variance from the AOR. The two primary disadvantages of using AOR to compute long-term trend are: (1) there is no computational norm for modelling the minimum time span equation, and (2) the results are sensitive to the choice of values selected to represent the measurement errors (Dolan et al. 1991). Foster and Savage (1989) do not suggest AOR as a general computational method but it can be used as a method of verification in combination with EPR and LR.

Linear regression

Linear regression is the most reliable method to predict future shoreline positions and their associated confidence intervals, if measurement errors and a linear trend of erosion were the only determining factors over the longest possible period of shoreline position (Crowell et al. 1997; Douglas and Crowell 2000). LR can reveal if an association exists, and in particular (via the R value), what fraction of the variance of the dependent variable (shoreline position) is attributable to the independent variable (time). This method uses all the available data from many datasets to find a line, which has the overall minimum of the squared distance to the known shoreline.

To calculate the rate of change and to predict the future shoreline position using LR, we have adopted the method established by Kumar et al. (2010b). The shoreline position (from SOI topographic maps) of 1910 has been chosen as a baseline or zero (0) position to measure the amount of shoreline shift. With reference to this baseline, progradation of the shoreline is considered as a positive value, while recession as a negative value. The change in shoreline position rate is calculated by the LR equation $y = \alpha + \beta t$, where y is the shoreline shift during the year t, with $y = 0$ for $t = 1910$. The regression coefficient (β) represents shoreline change rate and R is a measure of goodness-of-fit of the equation to the present data. In the present study, $R > 0.632$ has been chosen as the threshold of certainty for shoreline change rate calculation. The statistical significance is considered at the 80 % level of confidence (instead of 95 % confidence level) in view of small number of samples, as suggested by Allan et al. (2003).

Results and discussion

Shoreline configuration is commonly dynamic, exhibit temporal and spatial changes which are influenced by an accelerated or decelerated accretion of sediments along the coast. The complex interaction of a number of processes and factors such as magnitude of wave energy reaching the shoreline, secular sea-level changes, sediment supply and beach sediment budget, morphological properties are

responsible for recession of the shorelines (Amin and Davidson-Arnott 1997) while river flow and wave breakers play a significant role in shaping and orientating them (Kunte and Wagle 1991; Narayana and Priju 2006). Accelerated accretion or decelerated erosion results from greater sediment deposition, whereas decelerated accretion or accelerated erosion suggests greater sediment transport (Morton 1979). Further, shoreline changes of the Udupi coast are influenced by both the natural processes (waves, littoral currents, offshore relief, river mouth changes and sea-level changes) and anthropogenic activities (construction of coastal structures, sand mining and dredging of navigation channels) (Jayappa et al. 2003; Dwarakish et al. 2009; Kumar and Jayappa 2009). Past shoreline positions and rate of shoreline change, statistical results for selection of shoreline-rate measurement, prediction of future shoreline positions considering 1910 positions as base, role of correlation coefficient and RMSE on shoreline prediction and factors responsible for shoreline changes are explained below.

Past shoreline positions

The shoreline positions and changes in the last 98 years (1910–2008) indicate that all LCs are either subjected to progradation or recession during the different periods (1910–1967, 1967–1987, 1987–1992, 1992–1997, 1997–2001, 2001–2005 and 2005–2008), however, there is net recession in most of the transects from 1910 to 2008 (Fig. 2). Littoral cell-wise, the shoreline change rate for all transects has been calculated for 1910 as base year using EPR, AOR and LR methods (Table 2; Fig. 3). Variations in rate of change have been attributed to limited datasets, i.e., only one dataset is available during the period from 1910 to 1967, whereas after 1967, six available datasets were utilized for the present study.

Littoral cell-I

In this cell, shoreline along the transects Tr1.2–Tr1.5 and Tr1.20–Tr1.21 has receded during 1910–1967 with a maximum of 72 m (Tr1.21). Maximum shoreline progradation of ~200 m has been found in Tr1.17 during this period. During 1967–1987, most of the transects (except Tr1.13–Tr1.15) underwent recession with a maximum of ~210 m (Tr1.21), near the river mouth (Fig. 2). After 1987, most of the transects are subjected to minor recession and the remaining exhibit minor progradation. Transect Tr1.21 shows a progradation of ~120 m during 1987–1992 and ~135 m during 2001–2005. The net shoreline changes during 1910–2008 show recession at most of the transects (maximum in Tr1.7, i.e., 122 m) while progradation has been recorded in Tr1.12–Tr1.19 with a maximum of ~152 m (Tr1.17).

Based on the computed results of all three methods (EPR, AOR and LR), 59–63.64 % of transects of LC-I are subjected to erosion (Table 3). The river mouth of Udyavara near Tr1.22 has shifted ~500 m toward south during 1910–1987 but it again prograded by ~900 m during 1987–1992 and later minor changes have been noticed. Values of rate of shoreline changes calculated using AOR method are slightly different from those obtained from EPR and LR methods, during the last 98 year period (Fig. 3). Maximum rate of shoreline recession calculated by EPR and LR methods are 1.28 and 1.47 m/year, respectively, in the Tr1.5, whereas the maximum progradation rate is found in Tr1.17 for the last 98 years (Table 2).

Littoral cell-II

In this cell, shoreline recession is recorded in all the transects during 1910–1967 but it was severe near the Sita–Swarna rivers mouth (~177 m in Tr2.22). The river mouth has been shifted toward south by ~2.30 km and its width has been increased by ~100 m (400–500 m) during the last 98 years (Fig. 1). A small inlet has been formed near Tr.2.6 between 1910 and 1967. During 1967–1987 (except transects Tr2.1, Tr2.8–Tr2.11, Tr2.22 and Tr2.23), 17 transects out of 24 are subjected to recession with a maximum of ~170 m (Tr2.4). In the remaining periods, both recession and progradation patterns have been observed in all the transects except the Tr2.23 which shows a maximum recession of ~173 m during 1987–1992 (Fig. 2).

The net shoreline change during 1910–2008 shows that all the transects are under severe erosion with a maximum of ~240 m and the maximum rate of ~2.4 m/year at Tr2.23 (Table 2; Fig. 2). The shoreline rate calculated using AOR method is varying compared to that of EPR and LR methods. The rate of recession at most of the transects varies between 0.5 and 2.5 m/year (Fig. 3).

Littoral cell-III

In the last 98 years, 63–68.5 % of transects experience erosion with a maximum of ~170 m in Tr3.10 (Table 3). Out of 35 transects, only 12 shown progradation trend and at the remaining 23 transects, shoreline positions are receding with a maximum of ~150 m (Tr3.9 and Tr3.10) during 1910–1967. During 1967–87, shoreline recessions have been recorded in transects Tr3.2–Tr3.6, Tr3.28, Tr3.32–Tr3.35 with a maximum of ~120 m (Tr3.35). During 1987–2008, both recession and progradation trends are noticed in most of the transects (Fig. 2). The width of K–C–H rivers mouth was ~600 m during 1910 has been reduced to ~380 m by 2008. The river mouth has been shifted toward south by ~700 m in the last one century.

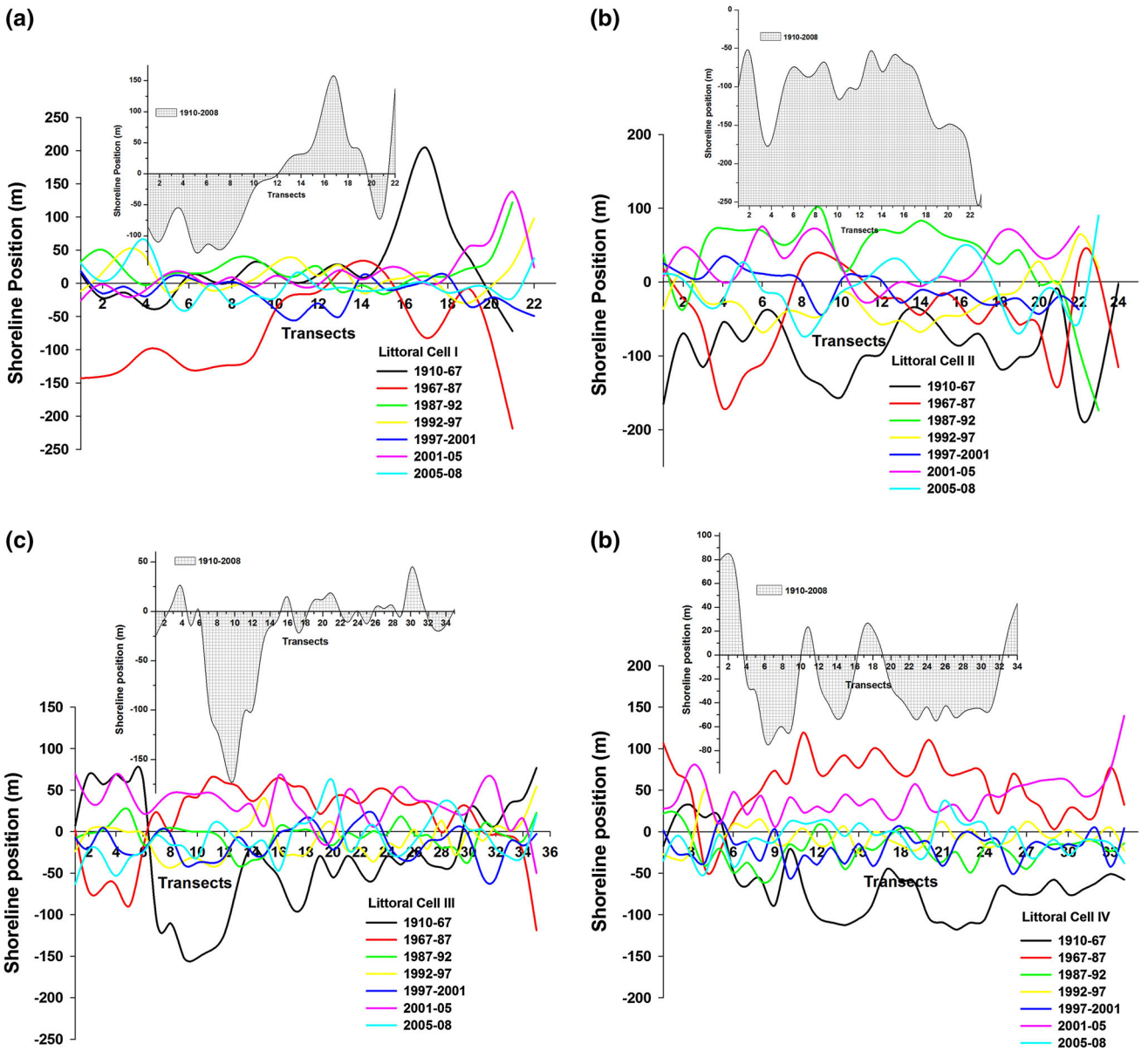

Fig. 2 Showing the periodical shorelines changes (1910–1967, 1967–1987, 1987–1992, 1992–1997, 1997–2001, 2001–2005 and 2005–2008) in all the littoral cells. The net change in the last 98 years is also shown

The shoreline change rate values obtained from different statistical methods show a maximum recession rate of ~1.7 m/year at Tr3.10 (Table 2, Fig. 3). The rate of shoreline recession has been considerably decreased in the long run while shoreline progradation rate has been increased in the last 48 years.

Littoral cell-IV

In this cell, all the transects, except Tr4.2–Tr4.5, show shoreline recession during 1910–1967. On the contrary, only Tr4.4 and Tr4.5 show shoreline recession during 1967–1987 and at other transects, shoreline prograded with a maximum of ~120 m (Tr4.11). From 1987 to 2001 period, shoreline positions at most of the transects are receded but during 2001–2005, all the transects experienced progradation with a maximum of ~140 m near Yedamavina Hole inlet (Tr4.34). Later, only ten transects are subjected to progradation and the remaining ones experienced recession (Fig. 2). From the computed results of EPR and LR methods, ~70 % transects of this cell are subjected to erosion with a maximum change of ~85 m at Tr4.6 in the last 98 years (Table 3). Maximum progradation of ~88 m has been noticed in Tr4.2. Maximum

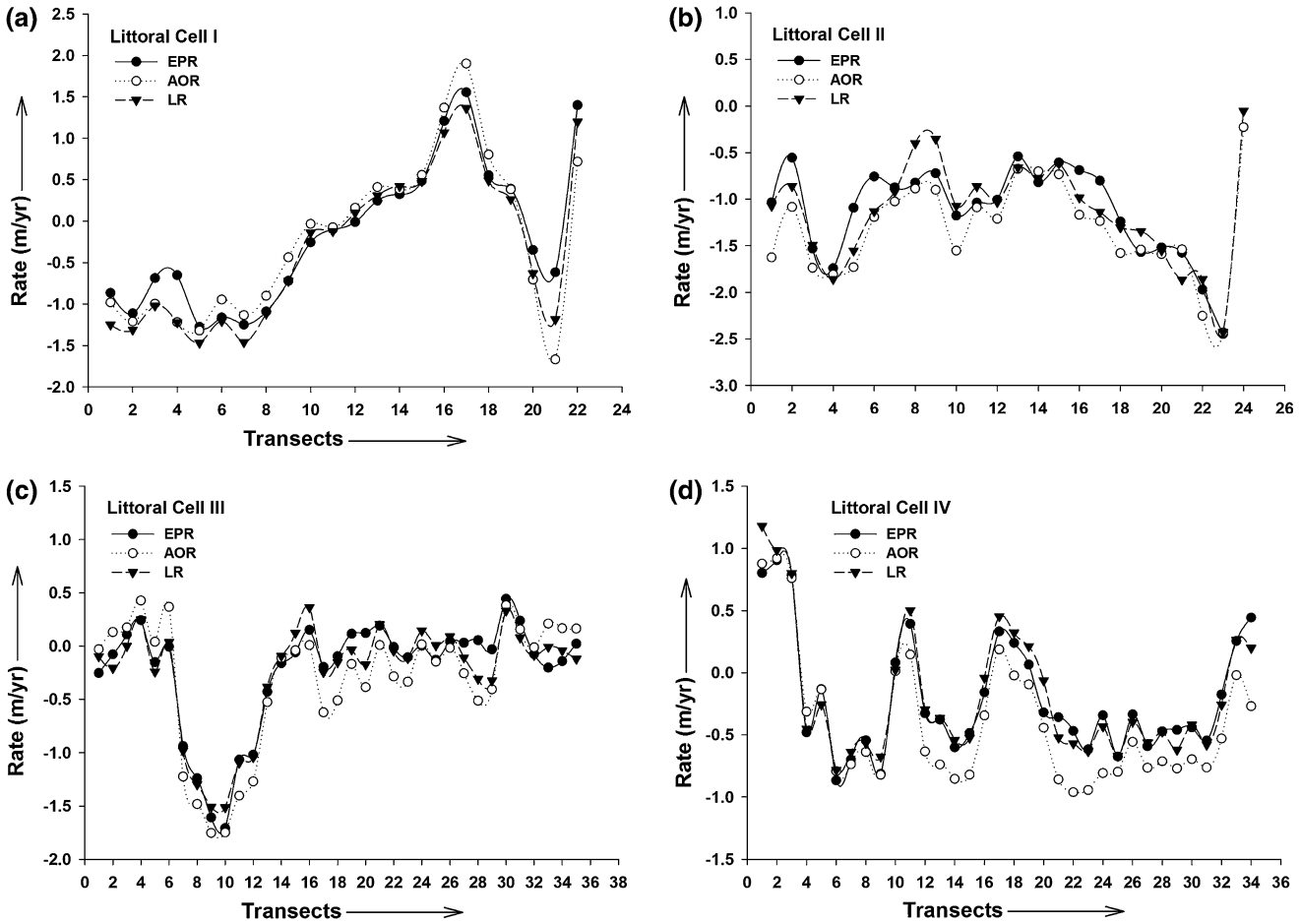

Fig. 3 Showing the shoreline change rate values calculated using EPR, AOR and LR methods for all the four littoral cells taking 1910 shoreline position as a base

shoreline recession rate of 0.8 m/year in Tr4.6 and progradation rate of 0.9 m/year in Tr4.2 are recorded (Table 2; Fig. 3). The rate of recession at most of the transects vary from 0.5 to 1.0 m/year, during 1910–2008 (Fig. 3).

Statistical results for the selection of shoreline change rate measurement

The rate of shoreline changes achieved by three different statistical methods has been compared with the values of LR vs. EPR and LR vs. AOR (Fig. 4). The diagonal line in the figure infers the possibilities between the two methods. The *R* value nearly one indicates the good relation among the independent and dependent variables. High degree of correlation between LR vs. EPR values were noticed as compared to that of LR vs. AOR in LC-I, -II and -IV whereas, in LC-II, good correlation between LR and AOR values are observed during 1910–2008 period (Fig. 4). The computed values of shoreline change rate obtained by LR and EPR methods are found to be close in all the LCs, therefore, these methods were used for the prediction of future shoreline positions. The computed results of LR method suggest that most of the transects in all the LCs have significant correlation coefficient (>0.63) (Table 3).

Predicted future shoreline positions

The future shoreline positions for 12 and 22 years, i.e., 2020 and 2030, respectively, were calculated with respect to the shoreline position of 2008 using EPR and LR models (Table 2). The results obtained by these two models do not seem to match exactly but ±10 m difference can be permissible due to different methods used in the estimation of rate of change in shoreline position. Hence, computed results of predicted shoreline position (for next 12 and 22 years) using LR method has been illustrated in Fig. 5.

In LC-I, the future predicted shoreline positions (for next 12 years) show recession (Tr1.1–Tr1.12 and Tr.1.20–Tr.1.21) and progradation (Tr1.13–Tr1.19 and Tr.22) with

Table 3 Total statistical summary of all the littoral cells of the study area during 1910–2008

Sl. no.	Shoreline statistics	LC-I	LC-II	LC-III	LC-IV	In-total
1	Total number of transects	22	24	35	34	115
2	Shoreline length (km)	11	13.5	18	17	59.5
3	Mean rate of shoreline change (m/year)					
	EPR	−0.18	−1.14	−0.23	−0.21	−0.40
	AOR	−0.23	−1.31	−0.31	−0.41	−0.53
	LR	−0.33	−1.13	−0.25	−0.19	−0.43
4	Minimum rate of shoreline change (m/year)					
	EPR	−0.01	−0.54	−0.01	0.07	−0.01
	AOR	−0.03	−0.23	−0.01	0.01	−0.01
	LR	−0.12	−0.05	−0.01	0.02	−0.01
5	Maximum rate of shoreline change (m/year)					
	EPR	1.55	−2.45	−1.71	0.90	−2.45
	AOR	1.90	−2.43	−1.75	−0.96	−2.43
	LR	1.36	−2.43	−1.51	1.18	−2.43
6	Standard deviation of shoreline change					
	EPR	0.86	0.49	0.52	0.47	0.69
	AOR	0.96	0.51	0.60	0.52	0.76
	LR	0.93	0.55	0.50	0.51	0.71
7	Total transects subjected to erosion					
	EPR	14	23	22	24	83
	AOR	13	24	22	28	87
	LR	13	24	24	24	85
8	Total transects subjected to accretion					
	EPR	8	0	13	10	31
	AOR	9	0	13	6	28
	LR	9	0	11	10	30
9	Total transects record statistical uncertainty ($R < 0.63$)	8	4	29	24	65
10	Total transects showing <10 m RMS error (for 11-year period)	10	12	18	21	61
11	Percentage of transects subjected to erosion					
	EPR	63.64	100.00	62.86	70.59	74.27
	AOR	59.09	100.00	62.86	82.35	76.08
	LR	59.09	100.00	68.57	70.59	74.56
12	Percentage of transects subjected to accretion					
	EPR	36.36	0	37.14	29.41	25.73
	AOR	40.91	0	37.14	17.65	23.92
	LR	40.91	0	31.43	29.41	25.44
13	Percentage of transects record statistical uncertainty ($R < 0.63$)	36.36	16.67	82.86	70.59	56.52
14	Percentage of transects showing <10 m RMS error (for 11 years period)	45.45	50.00	51.43	61.76	53.04
15	Cross-validation of 1997 (11 years past) RMS error (m) ($N = 115$)	19.48	22.14	14.27	12.65	16.86
16	Cross-validation of 1983 (23 years past) RMS error (m) ($N = 115$)	50.36	44.78	18.14	24.57	34.38
17	Predicted avg. shoreline shift amount (m) in 12 years					
	EPR	−19.98	−124.99	−24.90	−22.62	−43.46
	LR	−30.00	−136.09	−31.25	−34.36	−53.81
18	Predicted avg. shoreline shift amount (m) in 22 years (based on 2008)					
	EPR	−21.79	−136.35	−27.16	−24.68	−47.42
	LR	−33.25	−147.42	−33.70	−36.25	−58.10

N is total number of transects considered for individual periods; negative sign indicates erosion

respect to the shoreline position of 2008 (Table 2). The predicted shoreline positions of EPR and LR models validating accurately (error of ± 10 m) at transects Tr1.7–Tr1.8, Tr1.11, Tr1.14–Tr1.16 and Tr1.19 where the maximum recession and progradation were recorded in Tr1.7 (∼137 m) and Tr1.16 (∼132 m), respectively. However, in the next 22 years, predicted shoreline position exhibits similar recession and progradation trends whereas both the models validate accurately at transects Tr1.7, Tr1.8, Tr1.11, and Tr1.14–Tr1.19. In the case of Tr.12, the predicted shoreline models indicate two different trends for next 12- and 22-year periods. The predicted values obtained from EPR and LR models, EPR values show less compared to that of LR value. In total, about 60 % transects of this cell have been predicted to be subjected to recession (Table 2).

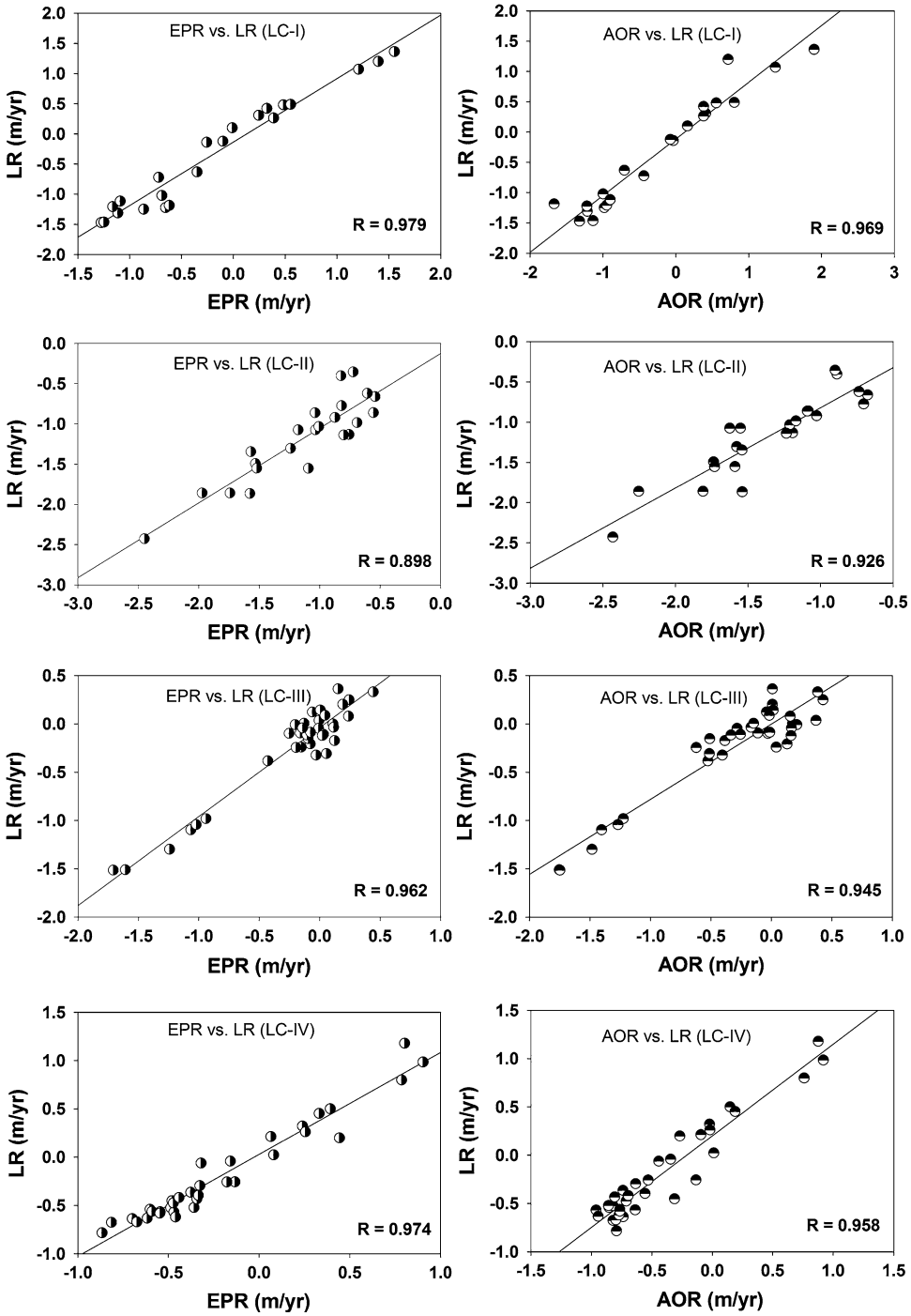

Fig. 4 Comparison of rate values computed by various methods for each transects taking 1910 shoreline position as a base. The *diagonal line* indicates the equivalence between the two methods and *R* values near 1 indicate good relation between the independent and dependent variables. Note that there is a high degree of correlation between LR vs. EPR compared to LR vs. AOR

In LC-II, prediction suggests that all the transects will continue recession trend for the next 12- and 22-year periods (Table 2). Out of 24 transects, only 6 (Tr2.9, Tr2.11, Tr2.14, Tr2.15, Tr2.20 and Tr2.23) confer identical values by EPR and LR models for both 12 and 22 years. Maximum erosion of ~270 m for 12 years and ~290 m for 22 years is predicted in Tr2.23 (Table 2). The EPR model is unable to predict the shoreline position of Tr2.24, whereas the LR model indicates change in shoreline for both 12 and 22 years.

In LC-III, the future shoreline positions show recession (Tr3.1–Tr3.2, Tr3.5, Tr3.7–Tr3.14, Tr3.17–Tr3.18, Tr3.22–Tr3.23, Tr3.25, Tr3.29 and Tr3.32) and progradation (Tr3.3–Tr3.4, Tr3.16, Tr3.21, Tr3.24, Tr3.26, Tr3.30–

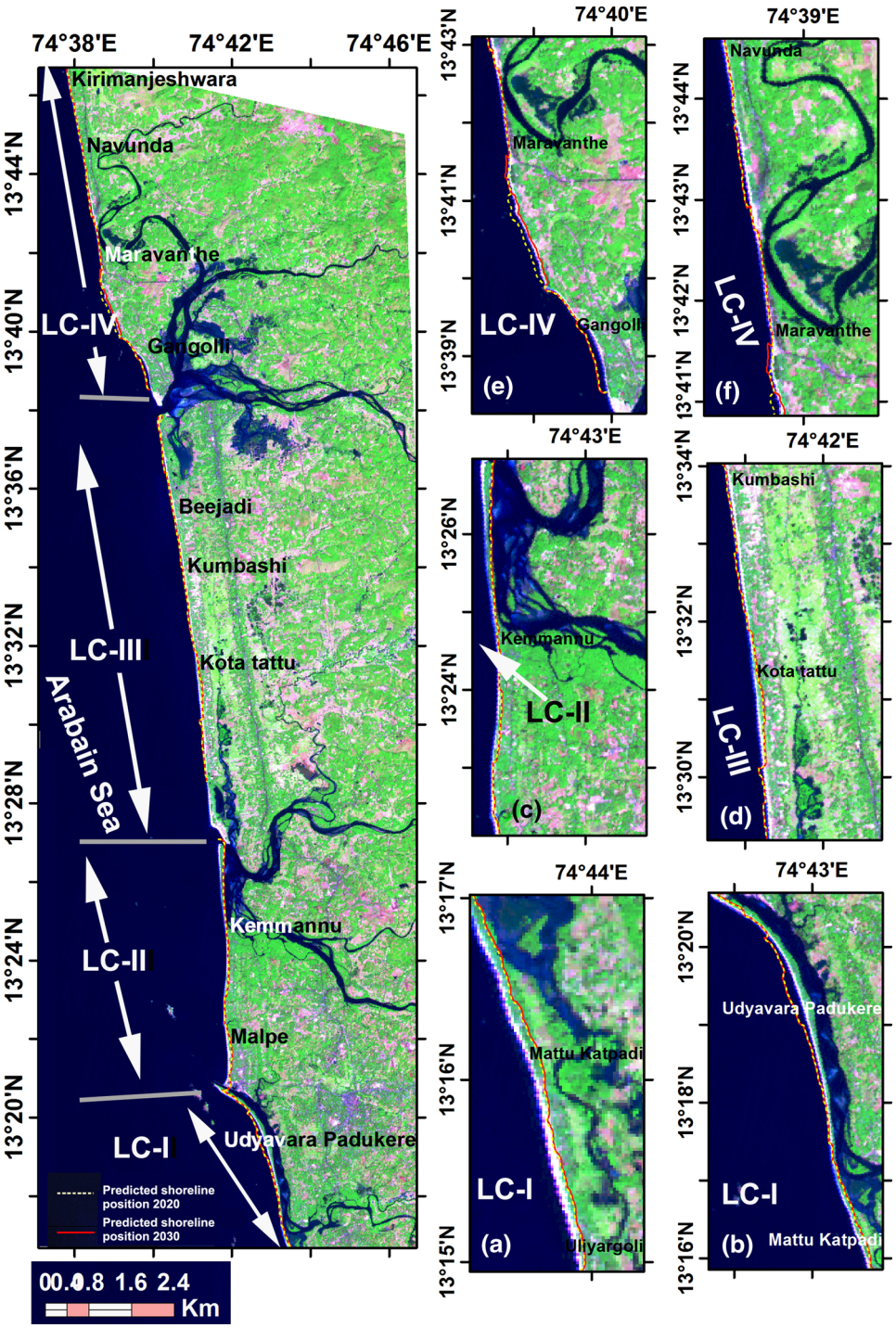

Fig. 5 Linear regression (LR) model predicted the shoreline position for 12- and 22-year periods, i.e., by 2020 (*dotted line*) and 2030 (*solid line*) with 2008 as base year is shown for all the four littoral cells (LC-I to LC-IV). Each littoral cell is enlarged and illustrated on the *right-hand side*. Erosional trends predicted between Uliyargoli and Mattu Katpadi coast in the LC-I (**a**). Further north between Mattu Katpadi to Udyavara Padukere of LC-I, major progradation with minor recession is predicted (**b**). The model suggests erosional trends for 12- and 22-year periods in LC-II (**c**). Alternate erosion and accretion trends have been predicted for the next 22-year periods in LC-III (**d**). Major progradation and recession trends have been predicted from Gangolli to Maravanthe and from Maravanthe to Kirimanjeshwara, respectively in LC-IV (**e**, **f**)

Tr3.31 and Tr3.35) trends for the next 12 years (Table 2). The EPR and LR models are validating the accurate shoreline position values of transects Tr3.2–Tr3.3, Tr3.5, Tr3.9–Tr3.10, Tr3.13–Tr3.14, Tr3.16, Tr3.24–Tr3.26, Tr3.30, Tr3.32 and Tr3.35 for the next 12 and 22 years. Computed values of EPR and LR models suggest that ~40 % of transects of LC-III will exhibit similar shoreline position. However, those transects which have showed shoreline recession and progradation trends for 12 years will be continued with the same trend for the next 22 years. Maximum recession of ~180 and ~200 m (at Tr3.10) and progradation of ~40 and ~50 m (at Tr3.30) are recorded for 12 and 22 years, respectively. For transects Tr3.6, Tr3.15, Tr3.33, Tr3.34, recession can be predicted for 12 and 22 years by EPR model, whereas LR model indicates progradation. On the contrary, for the transects Tr3.19, Tr3.20, Tr3.27 and Tr3.28, progradation and recession are predicted by EPR and LR models, respectively (Table 2).

In LC-IV, the future shoreline predictions for the next 12 and 22 years show recession at transects TR4.4–Tr4.9, Tr4.12–Tr4.16, Tr4.20–Tr4.32 and the remaining transects (except Tr4.34) show progradation. Transects Tr4.2, Tr4.3, Tr4.5–Tr4.10, Tr4.16, Tr4.17, Tr4.19, Tr4.20, Tr4.25 and Tr4.27 predict almost similar shoreline positions from EPR and LR models for 12 and 22 years, whereas transect Tr4.11 validates accurately for 22 years. Maximum shoreline recession of ~95 and ~100 m for 12 and 22 years, respectively, recorded at Tr4.6, whereas the maximum shoreline progradation of ~100 m for 12 years and ~110 m for 22 years is recorded for Tr4.2. The predicted shoreline positions by EPR and LR models indicate opposite trend for 12- and 22-year period at Tr4.34 (Table 2). Prediction for 12 and 22 years suggests ~70 % of transects of this littoral cell will exhibit erosion.

Role of correlation coefficient and RMSEs on shoreline prediction

The independent variable (time) does not allow any prediction of the dependent variables (shoreline positions) when the values of R equals 0, and can perfectly predict the future shoreline position when R is equal to 1. Uncertainty in the rate of shoreline change measurement has been recorded in all the four LCs (Table 2). In LC-I, during 1910–2008, correlation coefficient value is found to be ≥0.76 (i.e., 99 % significant level) at ten transects (Tr1.1, Tr1.2, Tr1.4–Tr1.8, Tr1.14–Tr1.16), whereas the R value is found to be ≥0.63 (95 significant level) at four transects (Tr1.3, Tr1.9, Tr1.17 and Tr1.22), and in the remaining eight transects, R is recorded <0.63 (Tables 2, 3). In total, ~66 % of the transects of this littoral cell show the significant accuracy in the prediction of the future shoreline positions (Table 3). In LC-II, R value is found to be ≥0.76 at 13 transects (Tr2.3–Tr2.5, Tr2.7, Tr2.11, Tr2.12, Tr2.16–Tr2.22) whereas it is ≥0.63 at 7 transects (Tr2.1, Tr2.2, Tr2.6, Tr2.10 and Tr2.13–Tr2.15) and R value in the remaining 4 transects is <0.63 (Table 2). The statistical computation reveals that about 83 % transects of this littoral cell are able to accurately predict the future shoreline positions (Table 3). In LC-III, five transects (Tr3.7–Tr3.10, Tr.3.12) show R value of >0.76 and only one transect (Tr3.11) shows >0.63 of R, whereas the remaining transects exhibit <0.63, during 1910–2008 (Table 2). In LC-IV, only nine transects (Tr4.1–Tr4.3, Tr4.6–Tr4.7, Tr4.9, Tr4.25, Tr4.29 and Tr4.31) exhibit the R value of >0.63 during 1910–2008 (Table 2). In total, uncertainties in shoreline prediction were found to be more in LC-III and LC-IV (82 and 73, respectively).

Out of 115 transects from all the four LCs, R value is found to be 95 significant level (≥0.63) at 50 transects, whereas the remaining 65 transects recorded comparatively less significant and higher uncertainty in prediction (Tables 2, 3). Highest number of transects (16) of LC-III compared to other LCs show $R \leq 0.2$ indicating the unpredictability in forecasting the future position. The uncertainties in R values are mainly observed in transects those are adjacent to estuaries, inlets, spits, breakwaters, ports and harbours.

RMSE is the difference between the desired output coordinate for a GCP and the actual output coordinate for the same point, when the point is transformed with the geometric transformation (ERDAS 2005). It is an indicator of the goodness-of-fit of the transformation to the selected GCPs, thus, it is only a crude indicator of positional accuracy throughout the image (White and El Asmar 1999). RMSE values estimated for the past shoreline changes (with respect to 2008 shoreline position), i.e., for 11 and 21 years, range from 0.16 (Tr3.9, LC-III) to 72.87 m (Tr2.23, LC-II) for 11-years and 0.64 (Tr3.8, LC-III) to 167.38 m (Tr1.21, LC-I) for 21-years during 1910–2008 (Table 2). For the 11-year period, 53 % of transects show <10 m RMS error, while for the 21-year period only 23 % transects show an error of <10 m (Table 2). In each littoral cell, the majority of transects show lower RMSE values for the 11-year period compared to that of 21-year period (Table 2). Littoral cell-wise RMSE estimation for 11- and 21-year periods is given in Table 3 to arrive at meaningful inferences with respect to geomorphological observations. RMSE values computed for the entire cell (all transects in each cell), it is observed that the values are less for 11-year period in all the four cells (Table 3). The results of RMSEs can be used to

understand the role and extent of natural processes and anthropogenic activities on shoreline changes. Taking into account the shoreline position of 1910 as base, most of transects of all the four LCs are predicted to exhibit erosion for 12 and 22 years (Tables 2, 3).

Shoreline changes due to coastal processes and monsoonal variation

Shoreline changes depend on the shoreline configuration, source and sink of sediment, and the hydrodynamics of the nearshore region. The wave-induced longshore currents produce spatial variations in the erosion/accretion pattern of beach and the wind induced circulation has a direct bearing (Rajith et al. 2008). Recession/progradation of shoreline is generally controlled by the temporal variability in the intensity and reversibility of wave directions and associated longshore currents, coastline orientation and by the existing coastal protection structures (Frihy et al. 2003). This coast is influenced by two monsoons: (1) the southwest (summer) monsoon (June–September) which is stronger than (2) the northeast (winter) monsoon (October–December). During southwest monsoon, the coastal current is stronger and sets-in clockwise direction, while during the northeast monsoon, it is in the counter-clockwise direction. As a result, littoral current in the study area are directed toward south during November–April when waves approach from WNW and NW directions and toward north from May–October when waves approach from SW, WSW and W directions (Hariharan et al. 1978; Narayana et al. 2001; Jayappa et al. 2003). Therefore, it is important to understand how sediments from various sources on the beaches are reworked and redistributed by the nearshore hydrodynamic processes. When, littoral drift is directed toward south and any construction acting as barrier to this drift results in erosion on the downdrift side. Any obstruction to littoral sediment transport due to the presence of natural headlands, shoals, man-made structures (breakwaters, seawalls, groynes), etc., the equilibrium profile of the natural beach is disturbed (Rao et al. 2009; El Banna and Hereher 2008).

Monsoonal rainfall is one of the important factors that control the coastal processes and determines the freshwater discharges through river systems along this coast. A strong relationship was reported between the variability of rainfall and sediment transport, where high sediment discharges are recorded with high rainfall (Syvitski and Morehead 1999; Avinash et al. 2012b). Further, high wave activity during intensive monsoon makes the sea rough, and erodes the sediment along the coast, resulting in change of the shoreline configuration. Whereas, the low rainfall results in the reduction of sediment supply to the coastal region. The recent study carried out by Kumar et al. (2010b) suggests that the rainfall (normal 4,000 mm) during the southwest monsoon (June to September) constitutes about 87 % of the annual rainfall. From the last 105 years (1900–2005), annual average rainfall data reveals that the rainfall was generally above normal (4,100 mm) during 1910–1934 and 1955–1964; however, the rainfall was below normal during 1934–1955. Excess rainfall was recorded during 1974–1984 and 1990–1997 and low rainfall during 1967–1974, 1984–1990 and 2000–2005 periods. The detritus, derived from the Sahyadri hill ranges and transported through midlands to the coastal area by the river systems during the monsoon season, nourishes the beaches along the coast. The low rainfall since 2000 would have resulted in reduction of sediment supply to the coastal area. In summary, the intensive monsoon rainfall and sediment supply from the hinterland influence the configuration and position of the shoreline.

During pre-monsoon season, surging, spilling and plunging breakers with the significant wave height of 1.2 m, whereas it goes up-to 1.5 m during post-monsoon season. However, maximum wave height of 4.0 m (further south off the coast of Mangalore) is observed during SW monsoon (Avinash et al. 2012a). In the monsoon season, the wind energy was observed to be much greater, resulting in larger amplitude waves and strong littoral currents. Infragravity and far infragravity edge waves, coupled with strong reflections and undertow, play an important role in the hydrodynamics along the southwest coast of India (Tatavarti et al. 1996). In addition, the larger and strong waves and undertow processes continuously disturb and erode the nearshore bed during monsoon season and therefore sediments are triggered into suspension and transported. As the low-frequency motions are three dimensional, they carry suspensions laterally (Tatavarti et al. 1999), thereby resulting in variations in shoreline positions. Although, large scale erosion takes place during the southwest monsoon, almost all the open beaches gradually start regaining the lost sand during post-monsoon season. But this balance is not found along the human intervened shorelines and at places interrupted by rock promontories or rivers mouth (Vijaya Kumar 2003). Interruption of longshore transport across the mouth of a river inlet is facilitated by the trapping of littoral sand to a varying extent by the inlet, resulting in reduced sand bypass to the down-drift shorelines. In other words, the inlets are sediment sinks at times (Fitzgerald 1988; Oertel 1988; Hayes 1991).

Impact of mean sea-level rise on shoreline configuration

Sea-level rises (SLRs) have direct impact on the shoreline changes which correspond to higher shift to the zone of

wave action on the beach. This would be reflected in a shoreline recession which will be larger on gentler slopes. Considerable interannual and interdecadal sea-level changes at a coast are forced primarily by large-scale winds (Clarke and Liu 1994; Shankar and Shetye 2001; Han and Webster 2002), large changes in salinity (Shankar and Shetye 1999; Shankar and Shetye 2001) as well as 'steric oscillations', which are due to the changes in specific volume (Shankar 2000). Bruun (1962) has developed a model which estimates the shoreline recession with respect to rise in sea level. If this model is considered for Karnataka coast, it suggests every millimetre rise of sea-level will result in a shoreline retreat of about 1 m (Dwarakish et al. 2009). Whereas, earlier studies reveal that there is a relative sea-level fall and SLR along the Mangalore coast, since the land is rising along the Mulky–Pulicat lake (MPL) axis close to 13°N latitude (Subrahmanya and Rao 1991). Dwarakish et al. (2009) have reported that the Udupi coast is vulnerable to susceptible SLR [59 % (very high risk), 7 % (high), 4 % (moderate) and 30 % (low vulnerable)] due to its low topography, high ecological and tourist value.

The estimated trends are consistent with the global estimates reported in the third assessment report (TAR) of

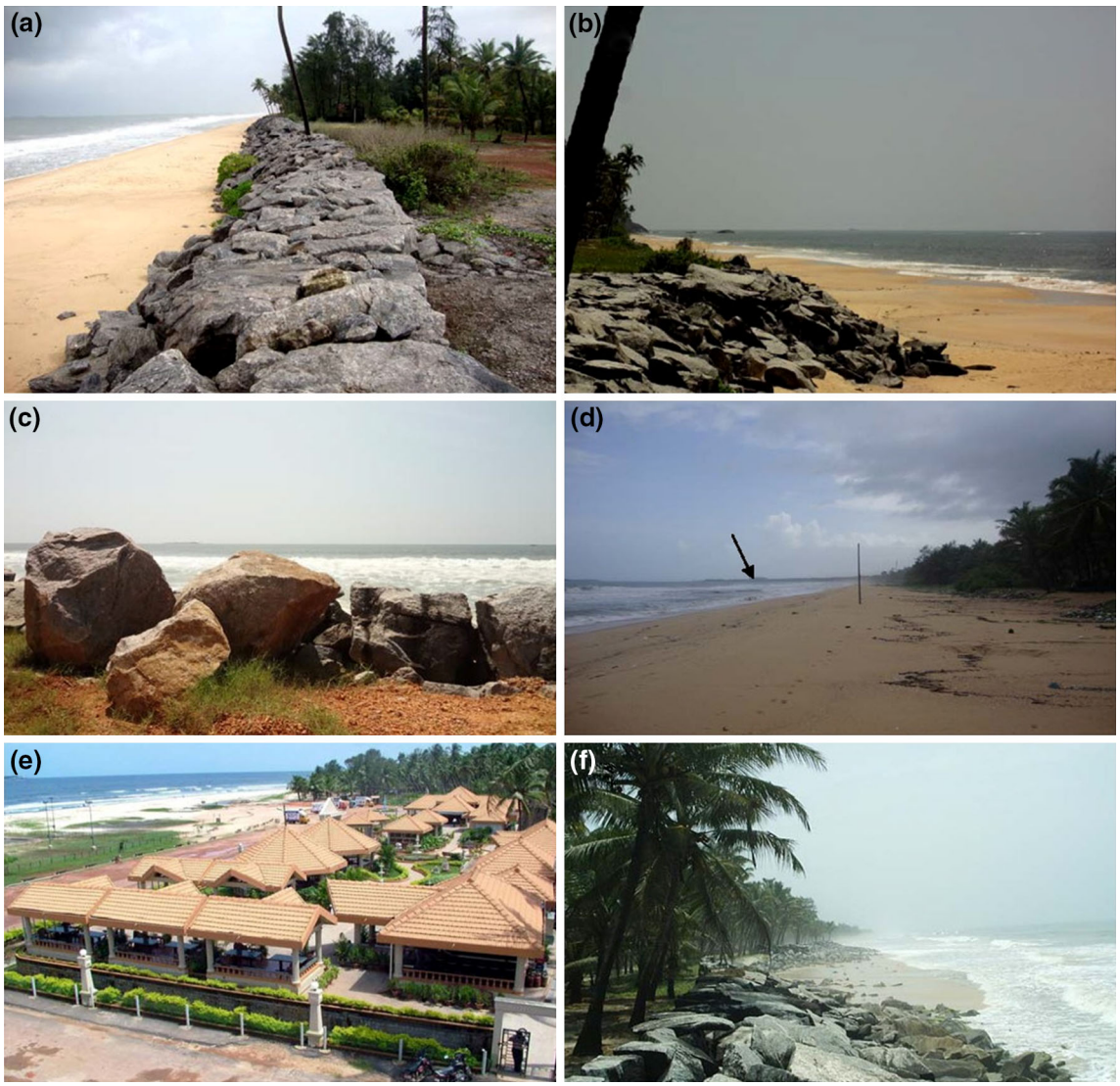

Fig. 6 **a** The beach near Uliyargoli (Tr1.1) is protected by seawall; **b** partially collapsed seawall near Uliyargoli; **c** dumped boulders to protect the beach from recession near Udyavara Padukere (Tr1.16); **d** breakwater construction on southern side of the Udyavara river mouth (Tr1.22); **e** tourist beach in Malpe (Tr2.2); Ipomoea—a sand binder is seen at the backshore; **f** severely eroding Kemmannu beach (Tr2.14)

Fig. 7 **a** A small inlet and seawalls are observed near Kumbhashi (Tr3.21); **b** organic shells extraction from the beach near Bijadi (Tr3.23); **c** sand dune in the hinterland near Saligrama (1 km away from the shoreline; Tr3.6); **d** severely eroding Maravanthe beach protected by seawalls (Tr4.20)

IPCC (Church et al. 2001), suggesting that the sea-level trends in the north Indian Ocean are comparable to global estimates. Over the globe, based on tide-gauge data, Douglas (2001), Church et al. (2004) and Holgate and Woodworth (2004) used reconstruction methods to determine the spatial pattern of global SLR of 1.8–2.0 mm/year during 1950–2000. These results were used to describe the regional sea-level changes and suggest values close to 2.0 mm/year in the north Indian Ocean, except the northeastern part of the Bay of Bengal, where values of >4 mm/year are found. The SLR variations suggest that the retreat along studied section may be gradually influencing and responsible for erosion. Hence, the Udupi coast is vulnerable to accelerated SLR and the rate of erosion of this coast during 2000–2006 was 0.6018 km^2/year compared to the rate of accretion and around 46 km of the coastline is under critical erosion (Dwarakish et al. 2009).

Shoreline changes due to anthropogenic activities

The presence of morphological structures on the shoreline results in seaward retreat of shoreline in the up-drift side and advances landward in the down drift side. Erosion/accretion is a cyclic phenomenon, which is normal along this coast. Beaches along the barrier spit are subjected to erosion due to migration of rivers mouth. Construction of breakwaters in 1980s on either side of Udyavara river mouth (LC-I and -II) results in significant growth of the southern spit. The change in beach configuration away from this estuarine mouth is influenced by St. Mary's group of islands situated in the offshore. Major shift of Sita–Swarna rivers mouth (LC-II and -III) toward south by ~2.30 km is recorded for the last 98 years, due to southerly drift which is predominating over northerly drift and coastal waves are stronger than river flow. Width of K–C–H rivers mouth (LC-IV) was ~600 m during 1910 has been reduced to ~380 m during 2008 which has been attributed to the construction of coastal engineering structures (Gangolli harbour, breakwaters and seawalls). Uliyargoli, Padukere, Vadabandeswara, Tonse, Kemmannu Hude, Parampalli and Kundapur Kodi are found as eroding beaches in the study area, whereas Kodi Bengre, Gangolli, Maravanthe beaches are highly vulnerable for erosion (Figs. 6, 7). A cumulative length of ~7 km seawalls has been con-

structed in the study area to protect the beaches from erosion, but most of them are partially destroyed.

Conclusion

Shoreline change analysis spanning 98 years along the Udupi coast supplemented by RS, GIS and statistical methods have contributed a better understanding of rates-of-change to evaluate spatial and temporal variability and to forecast future shoreline position to remediate the coast.

Shoreline change rates of Udupi coast estimated using EPR, AOR and LR methods suggest that the high degree of correlation between LR vs. EPR values were noticed as compared to that of LR vs. AOR. The investigation reveals high degree of correlation between LR and EPR methods, hence, these rates were used in the prediction of future shoreline positions. Correlation coefficient and RMSE are calculated to interpret the inaccuracies in rate and used in cross-validation of past shoreline positions. The results exhibit good agreement in values by EPR and LR models where the back calculated RMS error is $<$10 m. Lower RMSE value for the 11 year period compared to that of 21 year period in most of the transects is noticed. More uncertainty in shoreline predictions are recorded wherever the correlation coefficient is $<$0.2.

The study reports that the human interventions play a vital role in shoreline changes, in addition to natural processes. After the construction of breakwaters in 1980s on either side of Udyavara river mouth, significant growth ($\sim$45 m/year) of southern spit has been recorded. Major shift of Sita–Swarna rivers mouth toward south by $\sim$2.30 km is recorded due to the southerly drift. Width of Kollur–Chakra–Haladi rivers mouth which was $\sim$600 m during 1910 has been reduced to $\sim$380 m during 2008.

The cross-validated results indicate that the investigations for short-term (12 year period) are more reliable in estimating the shoreline positions for the regions affected by anthropogenic interventions; whereas, long-term (22 year period) studies can be used for reliable estimates of relatively stable or unaffected regions.

Acknowledgments The authors (DB and KSJ) thank the Ministry of Earth Sciences, New Delhi, India, for financial assistance through MMDP research project (No. MoES/11-MRDF/1/35/P/08-PC-III). The second author (AK) thanks Director, National Centre for Antarctic & Ocean Research (NCAOR) and Dr. John Kurian for their continuous support and encouragement. Authors also acknowledge anonymous reviewers and Editor-in-Chief of the Journal, for their insightful comments and suggestions on the previous draft, which improved the quality of the paper.

References

Abbas MH, Vishwanadham KD, Krishna Rao SVG (1991) Resource map of Udupi and Dakshina Kannada districts, Karnataka. Geological Survey of India, Hyderabad

Al Bakri D (1996) Natural hazards of shoreline bluff erosion: a case study of horizon view, Lake Huron. Geomorphology 17:323–337

Allan JC, Komar PD, Priest GR (2003) Shoreline variability on the high-energy Oregon Coast and its usefulness in erosion-hazard assessments. J Coast Res 38:83–105

Amin SMN, Davidson-Arnott RGD (1997) A statistical analysis of the controls on shoreline erosion rates, Lake Ontario. J Coast Res 13(4):1093–1101

Appeaning Addo K, Walkden M, Mills JP (2008) Detection, measurement and prediction of shoreline recession in Accra, Ghana. Photogram Remote Sens 63:543–558

Avinash Kumar, Jayappa KS, Vethamony P (2012a) Evolution of Swarna estuary and its impact on braided islands and estuarine banks, Southwest coast of India. Environ Earth Sci 65:835–848

Avinash Kumar, Jena B, Vinaya MS, Jayappa KS, Narayana, AC, Bhat HG (2012b) Regionally tuned algorithm to study the seasonal variation of suspended sediment concentration using IRS-P4 ocean colour monitor data. Egypt J Remote Sensing Space Sci 15:67–81. http://dx.doi.org/10.1016/j.ejrs.2012.05.003

Boak EH, Turner IL (2005) Shoreline definition and detection: a review. J Coast Res 21(4):688–703

Bray MJ, David JC, Janet MH (1995) Littoral cell definition and budgets for central southern England. J Coast Res 11(2):381–400

Bruun P (1962) Sea level rise as a cause of shore erosion. J Waterw Harb Div 88(1):117–130

Church JA, Gregory JM, Huybrechts M, Kuhn K, Lambeck MT, Nhuan Qin D, Woodworth PL (2001) Changes in sea level. Climate Change 2001: the scientific basis. Contribution of working group I to the third assessment report of the intergovernmental

Church JA, White NJ, Coleman R, Lambeck K, Mitrovica JX (2004) Estimates of regional distribution of sea level rise over the 1950–2000 period. J Climate 17:2609–2625

Clarke AJ, Liu X (1994) Interannual sea level in the northern and eastern Indian Ocean. J Geophys Res 99:1224–1235

Crowell M, Douglas BC, Leatherman SP (1997) On forecasting future US shoreline positions: a test of algorithms. J Coast Res 13(4):1245–1255

Dolan R, Fenster MS, Stuart JH (1991) Temporal analysis of shoreline recession and accretion. J Coast Res 7(3):723–744

Douglas BC (2001) Sea level change in the era of the recording tide gauge. In: Douglas BC, Kearney MS, Leatherman SP (eds) Sea level rise-history and consequences. Academic Press, New York, pp 37–64

Douglas BC, Crowell M (2000) Long-term shoreline position prediction and error propagation. J Coast Res 16(1):145–152

Douglas BC, Crowell M, Leatherman SP (1998) Considerations for shoreline position prediction. J Coast Res 14:1025–1033

Dwarakish GS, Vinay SA, Usha N, Toshiyuki A, Taro K, Katta Venkataramana B, Jagadeesha P, Babita MK (2009) Coastal vulnerability assessment of the future sea level rise in Udupi coastal zone of Karnataka state, west coast of India. Ocean Coast Manag 52:467–478

El Banna MM, Hereher ME (2008) Detecting temporal shoreline changes and erosion/accretion rates, using remote sensing, and their associated sediment characteristics along the coast of North Sinai. Egypt Environ Geol. doi:10.1007/s00254-008-1644-y

Eliot I, Clarke D (1989) Temporal and spatial bias in the estimation of shoreline rate-of-change statistics from beach survey information. Coast Manag 17:129–156

ERDAS (2005) ERDAS field guide. p 356
Fenster MS, Dolan R, Elder JF (1993) A new method for predicting shoreline positions from historical data. J Coast Res 9(1):147–171
Fitzgerald DM (1988) Shoreline erosional–depositional processes associated with tidal inlets. In: Aubrey DG, Weisher L (eds) Hydrodynamics and sediment dynamics of tidal inlets. Springer, New York, pp 186–225
Foster ER, Savage RJ (1989) Methods of historical shoreline analysis. In: Magoon OT, Converse H, Miner D, Tobin LT, Clark D (eds) Coastal zone'89, vol 5. American Society of Civil Engineers, Reston, pp 4434–4448
Frihy OE, Debes EA, El Sayed WR (2003) Processes reshaping the Nile delta promontories of Egypt: pre- and post-protection. Geomorphology 53:263–279
Gourlay MR (1996) Wave set-up on coral reefs. 2. Set-up on reefs with various profiles. Coast Eng 28:17–55
Han W, Webster PJ (2002) Forcing mechanisms of sea level interannual variability in the Bay of Bengal. J Phys Oceanogr 32:216–239
Hariharan V, Reddy MPM, Kurian NP (1978) Littoral and rip currents and beach profiles off Someshwar. Ind Geogr J 53:14–20
Hayes MO (1991) Geomorphology and sedimentation pattern of tidal inlets: a review. Coastal sediments'91, vol 2. ASCE, Reston, pp 1343–1355
Hengl T (2006) Finding the right pixel size. Comput Geosci 32:1283–1298
Holgate SJ, Woodworth PL (2004) Evidence for enhanced coastal sea level rise during the 1990s. Geophys Res Lett 31:L07305. doi: 10.1029/2004GL019626
Jantunen H, Raitala J (1984) Locating shoreline changes in the Porttipahta (Finland) water reservoir by using multitemporal Landsat data. Photogrammetria 39:1–12
Jayappa KS, Vijaya Kumar GT, Subrahmanya KR (2003) Influence of coastal structures on beach morphology and shoreline in Southern Karnataka, India. J Coast Res 19:389–408
Kumar A, Jayappa KS (2009) Long and short-term shoreline changes along Mangalore coast, India. Int J Environ Res 3:177–188
Kumar Avinash, Jayappa KS, Deepika B (2010a) Application of remote sensing and GIS in change detection of the Netravati and Gurpur river channels, Karnataka, India. Geocarto Int 25:397–425
Kumar Avinash, Narayana AC, Jayappa KS (2010b) Shoreline changes and morphology of spits along southern Karnataka, west coast of India: a remote sensing and statistics-based approach. Geomorphology 120:133–152
Kunte PD, Wagle BG (1991) Spit evolution and shore drift direction along South Karnataka coast, India. Giorn Geol 153:71–80
Lafon V, Froidefonda JM, Lahetb F, Castaing P (2002) SPOT shallow water bathymetry of a moderately turbid tidal inlet based on field measurements. Remote Sens Environ 81:136–138
Li R, Jung-Kuan Liu, Felus Y (2001) Spatial modelling and analysis for shoreline change detection and coastal erosion monitoring. Mar Geod 24:1–12
Maiti S, Bhattacharya AK (2009) Shoreline change analysis and its application to prediction: a remote sensing and statistics based approach. Mar Geol 257:11–23
Morton RA (1979) Temporal and spatial variations in shoreline changes and their implications, examples from the Texas Gulf Coast. J Sedi Petrol 49:1101–1112
Narayana AC, Priju CP (2006) Landform and shoreline changes inferred from satellite images along the central Kerala coast. J Geol Soc India 68:35–49
Narayana AC, Manojkumar P, Tatavarti R (2001) Beach dynamics related to the mudbank along the southwest coast of India. In: Mehta AJ, McAnally WH (eds) Coastal and estuarine fine sediment processes. Elsevier Science, BV, pp 495–507
Oertel GF (1988) Processes of sediment exchange between tidal inlets, ebb deltas and barrier islands. In: Aubrey DG, Weisher L (eds) Hydrodynamics and sediment dynamics of tidal inlets. Springer, New York, pp 297–318
Radhakrishna BP, Vaidyanadhan R (1994) Geology of Karnataka. Geological Society of India, Bangalore, pp 9–17
Rajith K, Kurian NP, Thomas KV, Prakash TN, Hameed TSS (2008) Erosion and accretion of a placer mining beach of SW Indian coast. Mar Geod 31:128–142
Rao VR, Ramana Murthy MV, Manjunath B, Reddy NT (2009) Littoral sediment transport and shoreline changes along Ennore on the southeast coast of India: Field observations and numerical modelling. Geomorphology 112:158–166
Ryu JH, Won JS, Min KD (2002) Waterline extraction from Landsat TM data in a tidal flat: a case study in Gosmo Bay, Korea. Remote Sens Environ 83:442–456
Scott DB (2005) Coastal changes, rapid. In: Schwartz ML (ed) Encyclopedia of coastal sciences. Springer, The Netherlands, pp 253–255
Shankar D (2000) Seasonal cycle of sea level and currents along the coast of India. Curr Sci 78:279–288
Shankar D, Shetye SR (1999) Are interdecadal sea level changes along the Indian coast influenced by variability of monsoon rainfall? J Geophys Res 104:26031–26041
Shankar D, Shetye SR (2001) Why is mean sea level along the Indian coast higher in the Bay of Bengal than in the Arabian Sea? Geophys Res Lett 28:563–565
Sherman DJ, Bauer BO (1993) Coastal geomorphology through the looking glass. Geomorphology 7:225–249
Siddiqui MN, Maajid S (2004) Monitoring of geomorphological changes for planning reclamation work in coastal area of Karachi, Pakistan. Adv Space Res 33:1200–1205
Singh A (1989) Digital change detection techniques using remotely sensed data. Int J Remote Sens 10:989–1003
SOI (Survey of India) (2007) Predicted tide table of Mangalore (Panambur), West Coast, India, pp 85–87
Subrahmanya KR, Rao BRJ (1991) Marine geological aspects of Dakshina Kannada coast: Perspective on Dakshina Kannada and Kodagu. Mangalore University Decennial Volume, Mangalore, pp 201–220
Syvitski JPM, Morehead MD (1999) Estimating river-sediment discharge to the ocean: application to the Eel margin, Northern California. Mar Geol 154:13–28
Tatavarti R, Narayana AC, Ravisankar M, Manojkumar P (1996) Mudbank dynamics: field evidence of edge waves and far infragravity waves. Curr Sci 38:837–843
Tatavarti R, Narayana AC, Manojkumar P, Shyam Chand P (1999) Mudbank regime of the Kerala coast during monsoon and non-monsoon seasons. Proc Ind Acad Sci 108:57–68
Vijaya Kumar GT (2003) A study of littoral processes and longshore sediment transport along the coast of Dakshina Kannada and Udupi districts, Karnataka. PhD Thesis (unpublished), Department of Marine Geology, Mangalore University, p 196
White K, El Asmar HM (1999) Monitoring changing position of coastlines using thematic mapper imagery, an example from the Nile Delta. Geomorphology 29:93–105
Yamano H, Shimazaki H, Matsunaga T, Ishoda A, McClennen C, Yokoki H, Fujita K, Osawa Y, Kayanne H (2006) Evaluation of

various satellite sensors for waterline extraction in a coral reef environment: Majuro Atoll, Marshall Islands. Geomorphology 82:398–411

Zuzek PJ, Nairn RB, Thieme SJ (2003) Spatial and temporal consideration for calculating shoreline change rates in the Great Lakes Basin. J Coast Res 38:125–146